Eur J Nucl Med Mol Imaging (2017) 44:979–987
DOI 10.1007/s00259-016-3605-0

ORIGINAL ARTICLE

Head-to-head comparison between ^{18}F-FDOPA PET/CT and MR/CT angiography in clinically recurrent head and neck paragangliomas

Céline Heimburger[1,2,3] · Francis Veillon[4] · David Taïeb[5,6,7] · Bernard Goichot[8] · Sophie Riehm[4] · Julie Petit-Thomas[9] · Gerlinde Averous[10] · Marcela Cavalcanti[4] · Fabrice Hubelé[1,2,3] · Gerard Chabrier[8] · Izzie Jacques Namer[1,2,3] · Anne Charpiot[9] · Alessio Imperiale[1,2,3,11]

Received: 11 October 2016 / Accepted: 20 December 2016 / Published online: 3 January 2017

Abstract
Purpose Head and neck paragangliomas (HNPGLs) can relapse after primary treatment. Optimal imaging protocols have not yet been established for posttreatment evaluation. The aim of the present study was to assess the diagnostic value of ^{18}F-FDOPA PET/CT and MR/CT angiography (MRA/CTA) in HNPGL patients with clinical relapse during their follow-up.
Methods Sixteen consecutive patients presenting with local pain, tinnitus, dysphagia, hoarse voice, cranial nerve involvement, deafness, or retrotympanic mass appearing during follow-up after the initial treatment of HNPGLs were retrospectively evaluated. Patients underwent both ^{18}F-FDOPA PET/CT and MRA (15 patents) or CTA (1 patent). Both methods were first assessed under blinded conditions and afterwards correlated. Head and neck imaging abnormalities without histological confirmation were considered true-positive results based on a consensus between radiologists and nuclear physicians and on further ^{18}F-FDOPA PET/CT and/or MRA.
Results ^{18}F-FDOPA PET/CT and MRA/CTA were concordant in 14 patients and in disagreement in 2 patients. ^{18}F-FDOPA PET/CT and MRA/CTA identified, respectively, 12 and 10 presumed recurrent HNPGLs in 12 patients. The two lesions diagnosed by PET/CT only were confirmed during follow-up by otoscopic examination and MRA performed 29 and 17 months later. ^{18}F-FDOPA PET/CT images were only slightly influenced by the posttreatment sequelae, showing a better interobserver reproducibility than MRA/CTA. Finally, in 2 of the 16 studied patients, ^{18}F-FDOPA PET/CT detected two additional synchronous primary HNPGLs.
Conclusion ^{18}F-FDOPA PET/CT is highly sensitive in posttreatment evaluation of patients with HNPGLs, and also offers better interobserver reproducibility than MRA/CTA and whole-body examination. We therefore suggest that ^{18}F-FDOPA PET/CT is performed as the first diagnostic imaging modality in symptomatic patients with suspicion of HNPGL relapse after primary treatment when ^{68}Ga-labeled somatostatin analogues are not available.

✉ Alessio Imperiale
alessio.imperiale@chru-strasbourg.fr

1 Department of Biophysics and Nuclear Medicine, University Hospitals of Strasbourg, Strasbourg, France
2 ICube, UMR 7357, CNRS/University of Strasbourg, Strasbourg, France
3 FMTS, Faculty of Medicine, University of Strasbourg, Strasbourg, France
4 Department of Radiology, University Hospitals of Strasbourg, Strasbourg, France
5 Department of Nuclear Medicine, La Timone University Hospital, Aix-Marseille University, Marseille, France
6 European Center for Research in Medical Imaging, Aix-Marseille University, Marseille, France
7 Inserm UMR1068 Marseille Cancerology Research Center, Institut Paoli-Calmettes, Marseille, France
8 Department of Internal Medicine, University Hospitals of Strasbourg, Strasbourg, France
9 Department of Otolaryngology and Maxillofacial Surgery, University Hospitals of Strasbourg, Strasbourg, France
10 Department of Pathology, University Hospitals of Strasbourg, Strasbourg, France
11 Biophysics and Nuclear Medicine, Hautepierre University Hospital, 1, Avenue Molière, 67098 Strasbourg Cedex, France

Keywords ^{18}F-FDOPA · Positron emission tomography · Paraganglioma · Magnetic resonance angiography · Recurrence · Head and neck

Introduction

Head and neck paragangliomas (HNPGLs) are neural crest-derived tumors associated with the parasympathic autonomic nervous system [1]. HNPGLs arise preferentially from paraganglia located in the jugular bulb, along the tympanic branch of the glossopharyngeal nerve, from the carotid body, or along the vagus nerve [2]. Up to 40% of HNPGLs are hereditary, most often related to a mutation in one of the genes encoding for the SDH complex [3–5]. Treatment is challenging and is tailored to each situation taking into account genetic status, tumor location and size, number of lesions, age, and comorbidities. Although surgery remains the main therapeutic option for Shamblin I/II carotid body PGL, observation and therapeutic radiation should be considered as first-line approaches for vagal and jugular PGL [6–8]. HNPGLs can relapse after the primary treatment. The recurrence rate is estimated to be 40–50% for jugular locations, 17% for PGL arising from the vagus nerve, and 10% for carotid body PGL [2].

Conventional MRI and ^{18}F-FDOPA PET/CT are currently recommended for initial evaluation of HNPGL [9, 10]. However, the imaging strategy for the diagnosis of recurrent HNPGLs has not yet been established. Three-dimensional (3D) time-of-flight (TOF) MR angiography (MRA) and contrast-enhanced 3D-MRA are highly informative with sensitivity and specificity of 90% and 92% [11], and 100% and 94% [12], respectively. More recently, the time-resolved imaging of contrast kinetics (4D-TRICKS) MRA has gained an increasing role in the evaluation of HNPGL [13]. ^{18}F-FDOPA PET/CT is highly sensitive (91%) and specific (95%) [14] and is currently performed as the first-line imaging modality in HNPGL [9, 10].

Detection of persistent/recurrent disease enables closer follow-up, and completion of radiation therapy or surgery [15, 16]. However, identification of tumor remnant or recurrence can be difficult mainly due to postoperative or radiation-induced morphological changes (e.g., fibrosis, edema, necrosis, or presence of surgical material) [17, 18]. Therefore, a functional diagnostic tool able to detect active disease with high sensitivity during the follow-up of treated HNPGL patients is mandatory to optimize the treatment of symptomatic patients with persistent/recurrent disease.

Accordingly, the primary aim of the present study was to determine the diagnostic value of ^{18}F-FDOPA PET/CT and MRA or CT angiography (CTA) in patients with a previous history of HNPGL who were asymptomatic after initial treatment but showed clinical recurrence during follow-up.

Materials and methods

Patients

The medical records of patients referred to the Nuclear Medicine Department of the Strasbourg University Hospital from November 2011 to April 2016 for a clinical symptomatology suggesting local evolution after initial treatment of HNPGL (local pain, tinnitus, dysphagia, hoarse voice, cranial nerve involvement, deafness, or retrotympanic mass) were retrospectively reviewed. Patients were included according to the following criteria: (1) MRA or CTA when MRA could not be performed, (2) ^{18}F-FDOPA PET/CT scan, and (3) clinical and radiological follow-up of at least 6 months after PET/CT imaging. Patients who did not undergo MRA or CTA or early head and neck PET/CT imaging were excluded.

Sixteen consecutive patients (12 women and 4 men; mean age 56.3 years, range 41–84 years) were retrospectively included (Table 1). The selected patients were symptomatic and previously treated for 18 HNPGLs located at the following sites: three involving the carotid body, ten glomus jugulare, two glomus tympanicum, and three glomus vagale tumors. Two patients were treated for synchronous bifocal disease: a bilateral glomus jugulare PGL in one patient and an association of one glomus vagale and one carotid body PGL in another patient. HNPGLs were initially treated as follows: complete surgical resection in 12 of 18 tumors, conventional fractionated radiation therapy in 4, and peptide receptor radionuclide therapy (PRRT) with ^{90}Y-DOTATOC in 2. Three of four HNPGLs previously treated with conventional fractionated radiation therapy showed almost complete regression on conventional morphological imaging performed early after the end of treatment. Finally, three HNPGLs treated with conventional fractionated radiation therapy (one patient) or PRRT (two patients) showed substantial fibrotic evolution on conventional imaging performed after irradiation and were finally considered as posttreatment sequelae because of a durable improvement in clinical symptomatology.

The mean time between the last treatment and ^{18}F-FDOPA PET/CT was 6.5 years (range 3 months to 28 years; median 1.3 years; 25th and 75th quartiles 7 months to 14 years). Six patients were *SDHx* mutation carriers (four *SDHB*, one *SDHC*, and one *SDHD*).

In keeping with local institutional guidelines, all patients gave written informed consent for the use of data extracted from their medical records for scientific or epidemiological purposes.

^{18}F-FDOPA PET/CT

^{18}F-FDOPA was used in the setting of an approved marketing authorization. All ^{18}F-FDOPA PET scans were performed using a combined PET/CT device. Patients fasted for at least

Table 1 Characteristics of the population studied

Patient no.	Sex	Age (years)	Genetics	Location of previously treated PGL	Previous treatment	Angiography	Angiography result	^{18}F-FDOPA PET/CT result	Final diagnosis	Size of recurrence (mm)	Follow-up (months)	Management of recurrences
1	F	53	SDHC	Right jugular	PRRT	3D-MRI (FGRE)	+	+	Recurrence	10	36	No treatment
2	M	50	Sporadic	Left carotid body	Surgery	CT	+	+	Recurrence	10	47	RT
3	F	63	Sporadic	Right jugulotympanic	RT	4D-MRI (TRICKS)	−	−	No recurrence		17	
				Left jugulotympanic	Surgery		−	+	Recurrence	11	17	No treatment
4	F	84	Sporadic	Left jugulotympanic	RT	4D-MRI (TRICKS)	+	+	Recurrence	30	18	No treatment
5	F	50	SDHD	Right carotid body	Surgery	3D-MRI (FGRE)	−	−	No recurrence		19	
6	F	68	Sporadic	Right tympanic	Surgery	4D-MRI (TRICKS)	−	−	No recurrence		11	
7	M	55	Sporadic	Right tympanic	Surgery	3D-MRI (FGRE)	−	+	Recurrence	10	29	RT
8	F	42	SDHB	Right glomus vagale	Surgery	4D-MRI (TRICKS)	−	−	No recurrence		9	
9	F	44	SDHB	Right glomus vagale	Surgery	3D-MRI (FGRE)	−	−	No recurrence		15	
				Left carotid	Surgery		−	−	No recurrence		15	
10	F	62	SDHB	Left glomus vagale	Surgery	3D-MRI (FGRE)	+	+	Recurrence	10	16	RT
11	F	70	Sporadic	Left jugulotympanic	RT	3D-MRI (FGRE)	+	+	Recurrence	13	12	No treatment
12	M	47	Sporadic	Left jugulotympanic	RT	3D-MRI (FGRE)	+	+	Recurrence	16	17	No treatment
13	F	59	Sporadic	Right jugulotympanic	PRRT	3D-MRI (FGRE)	+	+	Recurrence	18	25	No treatment
14	F	41	Sporadic	Right jugulotympanic	Surgery	3D-MRI (FGRE)	+	+	Recurrence[a]	18	−	Surgery
15	F	42	Sporadic	Right jugulotympanic	Surgery	4D-MRI (TRICKS)	+	+	Recurrence	22	9	RT
16	M	71	SDHB	Left jugular	Surgery	3D-MRI (FGRE)	+	+	Recurrence	8	10	No treatment

PRRT peptide receptor radionuclide therapy, *RT* conventional fractionated radiation therapy, *FGRE* fast gradient echo sequence, *TRICKS* time-resolved imaging of contrast kinetics

[a] Histological diagnosis

4 h before tracer injection. In all patients, 4 MBq/kg of ^{18}F-FDOPA was intravenously injected. No carbidopa premedication was used for any scan. ^{18}F-FDOPA PET/CT was performed using a dual-time acquisition protocol including an early acquisition (5–10 min after radiotracer injection) centered over the head and neck region (10 min per step) and a delayed whole-body acquisition (starting 30–40 min after radiotracer injection) from the top of the skull to the upper thigh (4 min per step) starting from the head. PET data were acquired using a matrix of 128 × 128 or 200 × 200 pixels. CT studies for attenuation correction and anatomic registration were performed without administration of contrast medium. PET data were reconstructed iteratively. CT, PET (after attenuation correction), and PET/CT images were displayed on a dedicated workstation for analysis.

A focal area of increased ^{18}F-FDOPA uptake in a usual anatomical site for paraganglia was considered a positive finding. In positive PET/CT studies, the tumor maximum standardized uptake value (SUV_{max}) was measured. Tumor SUV_{max} was defined within a spherical VOI centered on the tumor and including it completely. SUV_{mean} was considered for the background activity estimation by placing the same ROI on the normal contralateral region or on the cerebellum in patients with bilateral lesions. Hence, the tumor-to-background (T/B) ratio was estimated for each patient.

Radiological imaging

Head and neck MR investigations were performed with a 1.5-T (Avento; Siemens) or 3-T (Signa; General Electric) scanner. Morphological T1-weighted and T2-weighted axial and coronal images were acquired with a 1-mm slice thickness. Contrast-enhanced MRA was performed using either (a) a 3D fast gradient echo (3D-FGRE) sequence (FOV 20 × 16 cm, 256 × 256 matrix, TR 7.9 ms, TE 2.8 ms, slice thickness 0.8 mm) or (b) a 4D time-resolved imaging of contrast kinetics (4D-TRICKS) sequence (FOV 23 × 23 cm, 224 × 224 matrix, TR 3.8 ms, TE 2.1 ms, slice thickness 0.8 mm) with axial and coronal reconstructions. In patients in whom MRA was contraindicated, head and neck high-resolution CT and CTA were performed after administration of contrast medium in the arterial and venous phases (120 keV, 288 or 564 mAs, 0.6-mm slice thickness) with 3D reconstructions. A lesion detected in a usual anatomical site for paraganglia with classical imaging patterns of PGL was considered a positive finding.

Data analysis

^{18}F-FDOPA PET/CT and radiological imaging studies were independently reviewed by three nuclear physicians and three radiologists (two senior specialists and one resident from each specialty). Imaging results were interpreted as positive or negative for tumor recurrence and were thus compared head-to-head in each patient. Interpreting physicians were blinded to the other imaging results and clinical data except for the location of the previously treated HNPGLs. The imaging findings were considered concordant when they showed the same result. For the assessment of interobserver reproducibility, the ^{18}F-FDOPA PET/CT and radiological imaging studies were graded on a three-point scale: absence of tumor relapse, presence of PGL relapse, and inconclusive result.

Diagnostic criteria

When available, the pathological diagnosis of HNPGL was considered as the diagnostic gold standard for recurrence. However, histological proof of tumor recurrence was not attainable in all patients with positive imaging. Therefore, the results of ^{18}F-FDOPA PET/CT were systematically compared with the radiological imaging results. Both methods were first assessed under blinded conditions and correlated thereafter. All definite head and neck abnormalities localized with ^{18}F-FDOPA PET/CT and radiological imaging without histological confirmation were presumed to be true-positive lesions based on the worsening of clinical symptoms, the otoscopic results, and the following imaging results. During follow-up (mean follow-up period after imaging, 18.9 months, range, 9–47 months), the positive diagnosis was made by comparing the available imaging modalities (MRA, CT, ^{18}F-FDOPA PET/CT) and reaching a consensus between experienced radiologists and nuclear physicians. Finally, a definitive negative diagnosis of recurrent HNPGL was retained after spontaneous regression of clinical symptomatology and concordant negative imaging results without specific treatment within at least 9 months of follow-up.

Statistical analysis

The small number of patients included and the absence of a histological gold standard in the vast majority of patients prevented the calculation of sensitivity and specificity. Fleiss' kappa and Cohen's kappa coefficients were used to assess interobserver reproducibility. Kappa coefficients were interpreted using the benchmarks of Landis and Koch (0.81–1, almost perfect agreement; 0.61–0.8, substantial agreement; 0.41–0.6, moderate agreement; 0.21–0.4, fair agreement; 0.01–0.2, slight agreement). Tumor SUV_{max} and the T/B ratio were compared using Student's *t* test between patient groups (recurrent HNPGLs vs. untreated lesions) and within patient groups (early vs. delayed PET/CT). Statistical analysis was performed using the SPSS Statistics (IBM) software package. A p value less than 0.05 was considered significant.

Results

Imaging studies

Among the 16 patients included, all but one were evaluated by MRA, ten with 3D-FGRE sequences and five with 4D-TRICKS sequences. In the last patient MRA was contraindicated due to metallic surgical clips and this patient was therefore evaluated by contrast-enhanced high-resolution CTA. All patients underwent dual-time-point ^{18}F-FDOPA PET/CT. PET/CT and MRA/CTA were performed within a mean interval of 2 months (range 0–4 months) of each other.

Recurrence evaluation

Under blinded conditions, ^{18}F-FDOPA PET/CT and MRA/CTA were concordant in 14 patients (Fig. 1) and in disagreement in two patients (patients 3 and 7; Table 1). ^{18}F-FDOPA PET/CT identified 12 presumed recurrent HNPGLs in 12 patients. All lesions were easily detected by visual interpretation on both early and delayed PET/CT images. On the other hand, MRA/CTA detected ten presumed recurrences in ten patients. No presumed tumor detected by MRA/CTA was negative on ^{18}F-FDOPA PET/CT. MRA/CTA confirmed 10 of the 12 presumed tumors diagnosed by ^{18}F-FDOPA PET/CT. Concerning the two lesions diagnosed by PET/CT only, in one patient (patient 7) the correlation of ^{18}F-FDOPA PET/CT and MRA identified an irregular area of tissue measuring approximately 10 mm in the right jugulotympanic region without pathological enhancement, particularly in the early arterial phase (Fig. 2). In the second patient (patient 3) with a history of apparently sporadic bilateral jugulotympanic PGL, no MRA abnormalities corresponding to the focal ^{18}F-FDOPA uptake were found retrospectively in the left jugulotympanic region (Fig. 3). In both patients, recurrence was confirmed during follow-up by otoscopic examination and MRA performed 29 and 17 months later, respectively.

In four patients with presumed recurrent HNPGLs, whole-body PET/CT showed additional pathological ^{18}F-FDOPA uptake corresponding to a left carotid body PGL in one patient with an *SDHD* mutation (patient 5), a left carotid body PGL in one patient with an *SDHB* mutation (patient 8), metastatic bone

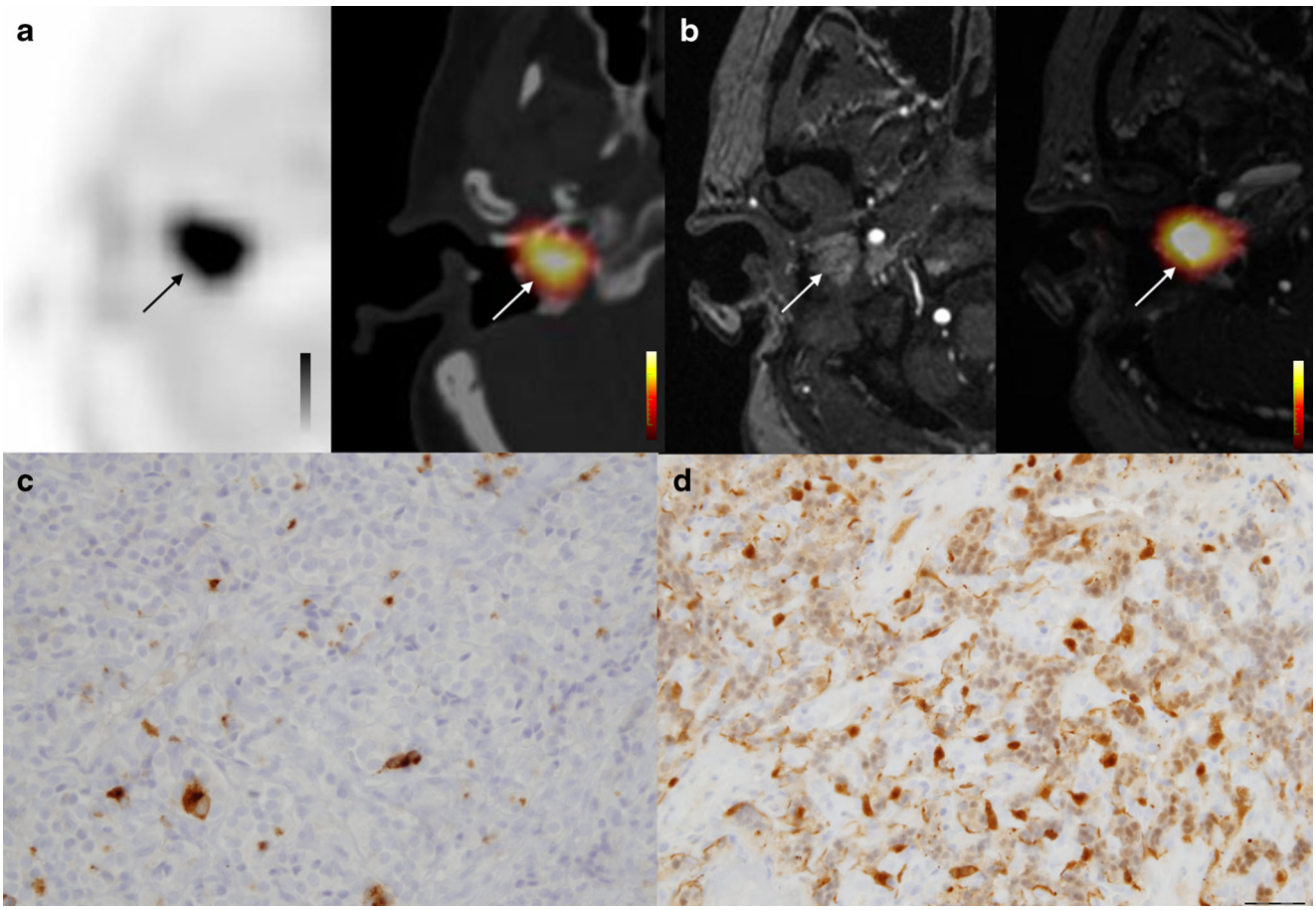

Fig. 1 A 41-year-old woman with a recurrent sporadic right jugulotympanic PGL treated by complete surgery (patient 14). **a** Axial PET and PET/CT images show intense ^{18}F-FDOPA uptake in the recurrent right jugulotympanic PGL. **b** Gadolinium-enhanced MRA image (3D-fast gradient echo sequence) shows typical enhancement of tumor relapse corresponding to 18F-FDOPA uptake on the PET and MRA fusion image. **c**, **d** Positive immunohistochemical staining (×400) for chromogranin-A (**c**) and PS-100 (**d**)

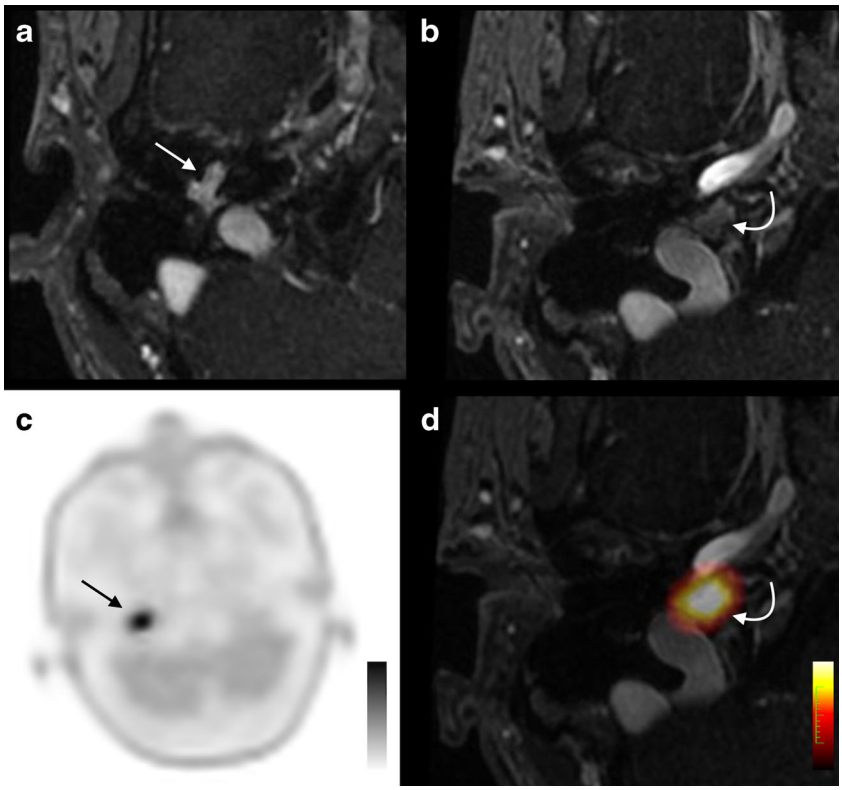

Fig. 2 A 55-year-old man with a history of apparently sporadic right tympanic PGL treated by complete surgery (patient 7). **a** Pretreatment axial gadolinium-enhanced MRA image (3D-fast gradient echo sequence, 3D-FGRE) shows intense and early enhancement of the right tympanic PGL. **b** Follow-up 3D-FGRE MRA image shows a heterogeneous area of tissue of diameter less than 10 mm in the right tympanic region without obvious enhancement. **c** Postsurgical axial ^{18}F-FDOPA PET image clearly shows tympanic tumor recurrence that was confirmed by 3D-FGRE MRA approximately 29 months later. **d** ^{18}F-FDOPA PET and MRA fusion image centered on the tumor recurrence

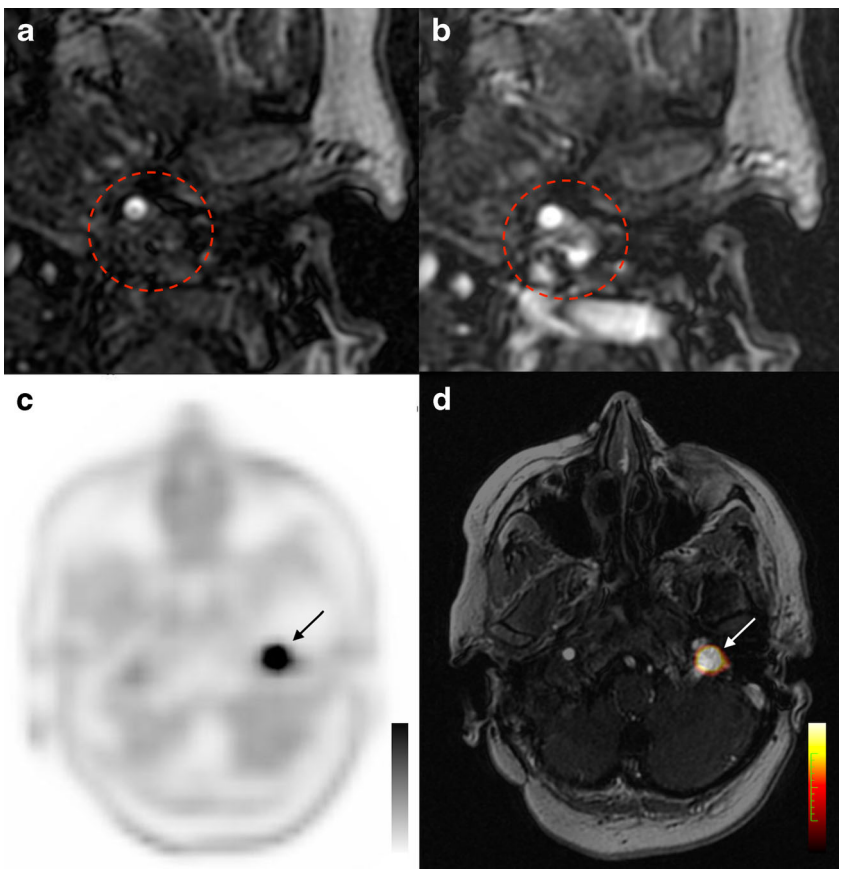

Fig. 3 A 63-year-old woman with a history of apparently sporadic bilateral jugulotympanic PGL successfully treated by external radiotherapy (right side) and surgery (left side) (patient 3). **a**, **b** Follow-up 4D time-resolved imaging of contrast kinetics (4D-TRICKS) MRA image shows no pathological findings in the left jugulotympanic region (*red dashed circle*), particularly in the early arterial phases. **c** Follow-up axial ^{18}F-FDOPA PET image clearly shows tumor recurrence of diameter 11 mm in the left jugulotympanic region that was confirmed by otoscopic examination 17 months later. **d** ^{18}F-FDOPA PET and MRA fusion image centered on the relapsing tumor

lesions in one patient with an *SDHB* mutation (patient 10), and a retroperitoneal PGL and a recurrent left jugular PGL in one patient with an *SDHB* mutation (patient 16). None of these tumors had previously been identified and were confirmed by subsequent imaging investigations and/or histological examination after surgery. Finally, a benign thyroid tumor with mild ^{18}F-FDOPA uptake was detected in one patient with an *SDHD* mutation (patient 5).

^{18}F-FDOPA uptake assessment

In the 12 presumed recurrent tumors, mean SUV_{max} values in early and delayed images were 27.8 ± 29.1 (range 3–87.7) and 20.9 ± 23.3 (range 2.7–82.8), respectively ($p = 0.29$). Mean T/B ratio values for the early and delayed images were elevated: 13.8 ± 11.3 (range 1.6–38.1) and 14 ± 13.7 (range 1.6–46), respectively ($p = 0.51$).

Interobserver reproducibility

The overall kappa coefficient was 0.59 (moderate agreement; 95% CI 0.38–0.79) for angiographic imaging and 0.92 (almost perfect agreement; 95% CI 0.67–1) for ^{18}F-FDOPA PET/CT. The interobserver reproducibility among the three referring physicians for both specialties was assessed by Cohen's kappa coefficient and is summarized in Table 2.

Tumor recurrence management

Of the 16 previously treated patients, presumed recurrent HNPGL was found in 12, and 7 of these 12 patients had been treated with surgery, three with conventional fractionated radiation therapy (delivered dose range 45–50 Gy at 1.8 Gy/fraction), and two with PRRT (2 × 100 mCi/m^2 body surface of ^{90}Y-DOTATOC). One recurrent tumor was located in the glomus vagale, one in the carotid body, nine in the glomus jugulare, and one in the glomus tympanicum (Table 1). Tumor recurrence was histologically proved in only one patient. The presumed tumor recurrence was treated surgically in one patient with relapsing PGL of the glomus jugulare (patient 14; Fig. 1) or with conventional fractionated radiation therapy in four patients, one with recurrent glomus vagale PGL, one with carotid body PGL, one with right tympanic PGL, and one with glomus jugulare (delivered dose range 45–60 Gy at 1.8–2 Gy/fraction; patients 2, 7, 10 and 15). No immediate treatment was recommended in the remaining seven patients.

Concerning the two patients diagnosed by PET/CT only, fractionated radiation therapy was indicated in one (patient 7). Treatment planning was done according to radiological and functional imaging. In the other patient (patient 3), a "wait and see" strategy was indicated despite the positive PET/CT finding.

Discussion

To the best of our knowledge, this is the first study evaluating the performance of ^{18}F-FDOPA PET/CT and MRA/CTA in patients with a history of HNPGL, who were asymptomatic after the initial treatment but presenting during follow-up with recurrent symptoms suggestive of local tumor evolution. Both techniques had high diagnostic performance in this clinical setting, but ^{18}F-FDOPA PET/CT seemed to be slightly superior to MRA/CTA in the identification of active disease.

Janssen et al. [19] and Archier et al. [20] prospectively compared ^{18}F-FDOPA PET/CT and CT/MRI in patients with HNPGL at primary staging. The sensitivity of ^{18}F-FDOPA PET/CT was better than that of conventional imaging in both studies. Similar results were obtained by Hoegerle et al. [21] using both ^{18}F-FDOPA PET/CT and conventional MRI in a series of ten consecutive patients with proven *SDHD* mutations. In that study, all tumors detected by MRI were also visualized by ^{18}F-FDOPA PET/CT. MRI, however, failed to identify four out of 14 presumed lesions detected by ^{18}F-FDOPA PET/CT. Marzola et al. [22] retrospectively studied ten consecutive patients with *SDHx* mutations investigated using ^{18}F-FDOPA PET/CT and conventional imaging. A total of 16 lesions were visualized by ^{18}F-FDOPA PET/CT, ten of which were located in the head and neck region, and only four were detected by CT/MRI. The limited utilization of MRA might explain the lower sensitivity of radiological imaging than ^{18}F-FDOPA PET/CT in the studies discussed above.

The 3D-TOF MRA acquisitions and 3D-MRA have been shown to be highly informative in the detection of HNPGL [11, 12]. The use of contrast-enhanced dynamic 3D-MRA leads to fewer image artifacts related to patient movement and blood flow, and provides dynamic information regarding

Table 2 Interobserver reproducibility among radiologists and nuclear medicine physicians

Interpreting physician	Radiology		Nuclear medicine	
	Cohen's kappa	95% CI	Cohen's kappa	95% CI
Senior specialist 1 vs. senior specialist 2	0.7	0.34–1	0.88	0.46–1
Senior specialist 1 vs. resident	0.54	0.2–0.88	1	0.54–1
Senior specialist 2 vs. resident	0.54	0.19–0.89	0.88	0.46–1

the arteriovenous circulation. However, the operator dependency of the method is not negligible. 4D-TRICKS MRA is an emergent and efficient technique [13]. TRICKS technology provides MRA imaging with remarkable spatial and temporal resolution. 4D-TRICKS offers time-resolved 3D images of blood vessels and captures the peak arterial phase with negligible venous pollution. With TRICKS, the different vascular phases can be rapidly separated and analyzed after image acquisition. However, iatrogenic modification of the regional anatomic architecture could be responsible for modification of the typical pattern of vascular and tissue enhancement after injection of contrast medium. The arrival of contrast medium during the early arterial phases could be delayed and less pronounced in irradiated lesions [23]. This phenomenon is potentially responsible for the incorrect interpretations, particularly in patients with considerable radiotherapy after-effects (Fig. 3). Hence, the clinical experience of the referring physician played a major role in morphological imaging analysis in this study. We found lower interobserver reproducibility among radiologists than nuclear physicians. On the other hand, the level of concordance for ^{18}F-FDOPA PET/CT image interpretation was excellent and the analysis of PET/CT images was only slightly influenced by posttreatment sequelae.

The identification of multifocality and local recurrence is crucial in patients with HNPGL for therapeutic optimization. In the present series, five patients with presumed recurrence underwent new treatment including surgery, radiation therapy, or a combination of both. Radiation therapy provides excellent local control of vagal and jugular PGL [1, 7, 24–28], with a change in the therapeutic paradigm in the event of tumor progression [6, 7]. The tumor regression rate is estimated at 64% in salvage conditions. Xerostomia, stenosis of the external auditory canal, and osteoradionecrosis of the temporal bone are possible late complications [7, 26]. When surgery or external radiotherapy are not indicated, PRRT using ^{90}Y/^{177}Lu-labeled somatostatin analogs is a therapeutic option suitable for metastatic HNPGL [19, 27, 28].

According to our experience, early head and neck PET/CT acquisitions provided no additional information. Therefore, we suggest that early head and neck PET/CT imaging is perfomed only in patients with a hereditary syndrome predisposed to developing medullary thyroid carcinoma. Our results also suggest that patients with sporadic recurrent HNPGLs could benefit from ^{18}F-FDOPA PET/CT as first-line imaging when clinical symptomatology appears after effective primary treatment and ^{68}Ga-DOTATATE PET/CT is not available [20, 21]. If ^{18}F-FDOPA PET/CT is positive, a conventional imaging approach could complete the diagnostic investigation to better define the following therapeutic strategy.

^{18}F-FDOPA PET/CT offers an additional advantage over MRA/CTA, including highly sensitive whole-body examination. In our population, ^{18}F-FDOPA whole-body PET/CT detected progressive head and neck disease after primary treatment, distant metastases and HNPGL multifocality. In this regard, PET/MRI seems particularly attractive, allowing in a single examination the detection of HNPGLs, and the assessment of tumor local extension and metastatic spread, which are essential for planning optimal treatment tailored to each clinical situation, and also exposes the patient to a lower radiation dose. Moreover, magnetic resonance spectroscopy could also be performed in the same session to detect specific metabolic biomarkers of pheochromocytoma and PGL [29, 30].

Despite these useful results, this study had the inherent limitations of any retrospective observational case series focused on a rare condition. The small population studied allowed no real statistical analysis; thus our findings must be considered as preliminary and need confirmation in larger series of patients. Furthermore, the genetic heterogeneity (*SDHx*-related and apparently sporadic tumors) of the selected patients may have been a potential bias in the interpretation of the results. Moreover, only one histologically confirmed recurrence was found because of the high morbidity associated with a second surgical procedure that occurred in several patients with positive HNPGL imaging.

In conclusion, ^{18}F-FDOPA PET/CT is highly sensitive in posttreatment evaluation of HNPGL. ^{18}F-FDOPA PET/CT offers distinct advantages over radiological imaging including better interobserver reproducibility and highly sensitive whole-body examination. In symptomatic patients with suspicion of tumor relapse after primary treatment, we suggest that ^{18}F-FDOPA PET/CT be used as the first diagnostic imaging modality to optimize the therapeutic strategy, particularly when PET/CT with ^{68}Ga-radiolabeled somatostatin analogs is not available.

Compliance with ethical standards

Conflicts of interest None.

Ethical approval All procedures performed in studies involving human participants were in accordance with the ethical standards of the institutional and/or national research committee and with the principles of the 1964 Declaration of Helsinki and its later amendments or comparable ethical standards.

Informed consent Informed consent was obtained from all individual participants included in the study.

References

1. Taïeb D, Kaliski A, Boedeker CC, Martucci V, Fojo T, Adler JR, et al. Current approaches and recent developments in the management of head and neck paragangliomas. Endocr Rev. 2014;35:795–819.

2. Rao AB, Koeller KK, Adair CF. From the archives of the AFIP. Paragangliomas of the head and neck: radiologic-pathologic correlation. Radiographics. 1999;19:1605–32.
3. Piccini V, Rapizzi E, Bacca A, Di Trapani G, Pulli R, Giachè V, et al. Head and neck paragangliomas: genetic spectrum and clinical variability in 79 consecutive patients. Endocr Relat Cancer. 2012;19:149–55.
4. Baysal BE, Willett-Brozick JE, Lawrence EC, Drovdlic CM, Savul SA, McLeod DR, et al. Prevalence of SDHB, SDHC, and SDHD germline mutations in clinic patients with head and neck paragangliomas. J Med Genet. 2002;39:178–83.
5. Neumann HP, Erlic Z, Boedeker CC, Rybicki LA, Robledo M, Hermsen M, et al. Clinical predictors for germline mutations in head and neck paraganglioma patients: cost reduction strategy in genetic diagnostic process as fall-out. Cancer Res. 2009;69:3650–56.
6. Wanna GB, Sweeney AD, Haynes DS, Carlson ML. Contemporary management of jugular paragangliomas. Otolaryngol Clin N Am. 2015;48:331–41.
7. Moore MG, Netterville JL, Mendenhall WM, Isaacson B, Nussenbaum B. Head and neck paragangliomas: an update on evaluation and management. Otolaryngol Head Neck Surg. 2016;154:597–605.
8. van Essen M, Krenning EP, Kooij PP, Bakker WH, Feelders RA, de Herder WW, et al. Effects of therapy with [177Lu-DOTA0, Tyr3]Octreotate in patients with paraganglioma, Meningioma, small cell lung carcinoma, and melanoma. J Nucl Med. 2006;47:1599–606.
9. Taïeb D, Timmers HJ, Hindié E, Guillet BA, Neumann HP, Walz MK, et al. EANM 2012 guidelines for radionuclide imaging of phaeochromocytoma and paraganglioma. Eur J Nucl Med Mol Imaging. 2012;39:1977–95.
10. Lenders JW, Duh QY, Eisenhofer G, Gimenez-Roqueplo AP, Grebe SK, Murad MH, et al. Pheochromocytoma and paraganglioma: an Endocrine Society clinical practice guideline. J Clin Endocrinol Metab. 2014;99:1915–42.
11. Neves F, Huwart L, Jourdan G, Reizine D, Herman P, Vicaut E, et al. Head and neck paragangliomas: value of contrast-enhanced 3D MR angiography. AJNR Am J Neuroradiol. 2008;29:883–9.
12. van den Berg R, Schepers A, de Bruïne FT, Liauw L, Mertens BJ, van der Mey AG, et al. The value of MR angiography techniques in the detection of head and neck paragangliomas. Eur J Radiol. 2004;52:240–45.
13. Arnold SM, Strecker R, Scheffler K, Spreer J, Schipper J, Neumann HP, et al. Dynamic contrast enhancement of paragangliomas of the head and neck: evaluation with time-resolved 2D MR projection angiography. Eur Radiol. 2003;13:1608–11.
14. Treglia G, Cocciolillo F, de Waure C, Di Nardo F, Gualano MR, Castaldi P, et al. Diagnostic performance of 18F-dihydroxyphenylalanine positron emission tomography in patients with paraganglioma: a meta-analysis. Eur J Nucl Med Mol Imaging. 2012;39:1144–53.
15. Elshaikh MA, Mahmoud-Ahmed AS, Kinney SE, Wood BG, Lee JH, Barnett GH, et al. Recurrent head-and-neck chemodectomas: a comparison of surgical and radiotherapeutic results. Int J Radiat Oncol Biol Phys. 2002;52:953–6.
16. Jackson CG, Harris PF, Glasscock ME, Fritsch M, Dimitrov E, Johnson GD, et al. Diagnosis and management of paragangliomas of the skull base. Am J Surg. 1990;159:389–93.
17. Ng SH, Joseph CT, Chan SC, Ko SF, Wang HM, Liao CT, et al. Clinical usefulness of 18F-FDG PET in nasopharyngeal carcinoma patients with questionable MRI findings for recurrence. J Nucl Med. 2004;45:1669–76.
18. Imperiale A, Riehm S, Braun JJ. Interest of [18F]FDG PET/CT for treatment efficacy assessment in aggressive phenotype of sarcoidosis with special emphasis on sinonasal involvement. Q J Nucl Med Mol Imaging. 2013;57:177–86.
19. Janssen I, Chen CC, Taieb D, Patronas NJ, Millo CM, Adams KT, et al. 68Ga-DOTATATE PET/CT in the localization of head and neck paragangliomas compared with other functional imaging modalities and CT/MRI. J Nucl Med. 2016;57:186–91.
20. Archier A, Varoquaux A, Garrigue P, Montava M, Guerin C, Gabriel S, et al. Prospective comparison of (68)Ga-DOTATATE and (18)F-FDOPA PET/CT in patients with various pheochromocytomas and paragangliomas with emphasis on sporadic cases. Eur J Nucl Med Mol Imaging. 2016;43:1248–57.
21. Hoegerle S, Ghanem N, Altehoefer C, Schipper J, Brink I, Moser E, et al. 18F-DOPA positron emission tomography for the detection of glomus tumours. Eur J Nucl Med Mol Imaging. 2003;30:689–94.
22. Marzola MC, Chondrogiannis S, Grassetto G, Rampin L, Maffione AM, Ferretti A, et al. 18F-DOPA PET/CT in the evaluation of hereditary SDH-deficiency paraganglioma-pheochromocytoma syndromes. Clin Nucl Med. 2014;39:e53–e58.
23. Handel SF, Miller MH, Miller LS, Goepfert H, Wallace S. Angiographic changes of head and neck chemodectomas following radiotherapy. Arch Otolaryngol 1960. 1977;103:87–9.
24. Cummings BJ, Beale FA, Garrett PG, Harwood AR, Keane TJ, Payne DG, et al. The treatment of glomus tumors in the temporal bone by megavoltage radiation. Cancer. 1984;53:2635–40.
25. Spector GJ, Maisel RH, Ogura JH. Glomus jugulare tumors. II. A clinicopathologic analysis of the effects of radiotherapy. Ann Otol Rhinol Laryngol. 1974;83:26–32.
26. Anttila T, Häyry V, Nicoli T, Hagström J, Aittomäki K, Vikatmaa P, et al. A two-decade experience of head and neck paragangliomas in a whole population-based single centre cohort. Eur Arch Otorhinolaryngol. 2015;272:2045–53.
27. Dupin C, Lang P, Dessard-Diana B, Simon JM, Cuenca X, Mazeron JJ, et al. Treatment of head and neck paragangliomas with external beam radiation therapy. Int J Radiat Oncol Biol Phys. 2014;89:353–9.
28. van Hulsteijn LT, Corssmit EP, Coremans IE, Smit JW, Jansen JC, Dekkers OM. Regression and local control rates after radiotherapy for jugulotympanic paragangliomas: systematic review and meta-analysis. Radiother Oncol. 2013;106:161–8.
29. Imperiale A, Battini S, Averous G, Mutter D, Goichot B, Bachellier P, et al. In vivo detection of catecholamines by magnetic resonance spectroscopy: a potential specific biomarker for the diagnosis of pheochromocytoma. Surgery. 2016;159:1231–33.
30. Varoquaux A, le Fur Y, Imperiale A, Reyre A, Montava M, Fakhry N, et al. Magnetic resonance spectroscopy of paragangliomas: new insights into in vivo metabolomics. Endocr Relat Cancer. 2015;22:M1–M8.